THE JOURNAL OF BIOLOGICAL CHEMISTRY
Vol. 278, No. 42, Issue of October 17, pp. 40890–40898, 2003

Printed in U.S.A.

Inactivation of Kv3.3 Potassium Channels in Heterologous Expression Systems*

Received for publication, April 22, 2003, and in revised form, August 11, 2003
Published, JBC Papers in Press, August 15, 2003, DOI 10.1074/jbc.M304235200

Fernando R. Fernandez‡, Ezequiel Morales‡, Asim J. Rashid§, Robert J. Dunn§, and Ray W. Turner‡¶

From the ‡Neuroscience Research Group, University of Calgary, Calgary, Alberta T2N 4N1, Canada and the §Departments of Neurology and Biology, McGill University, and Center for Research in Neuroscience, Montreal General Hospital, Montreal, Quebec H3G 1A4, Canada

Kv3.3 K^+ channels are believed to incorporate an NH_2-terminal domain to produce an intermediate rate of inactivation relative to the fast inactivating K^+ channels Kv3.4 and Kv1.4. The rate of Kv3.3 inactivation has, however, been difficult to establish given problems in obtaining consistent rates of inactivation in expression systems. This study characterized the properties of AptKv3.3, the teleost homologue of Kv3.3, when expressed in Chinese hamster ovary (CHO) or human embryonic kidney (HEK) cells. We show that the properties of AptKv3.3 differ significantly between CHO and HEK cells, with the largest difference occurring in the rate and voltage dependence of inactivation. While AptKv3.3 in CHO cells showed a fast and voltage-dependent rate of inactivation consistent with N-type inactivation, currents in HEK cells showed rates of inactivation that were voltage-independent and more consistent with a slower C-type inactivation. Examination of the mRNA sequence revealed that the first methionine start site had a weak Kozak consensus sequence, suggesting that the lack of inactivation in HEK cells could be due to translation at a second methionine start site downstream of the NH_2-terminal coding region. Mutating the nucleotide sequence surrounding the first methionine start site to one more closely resembling a Kozak consensus sequence produced currents that inactivated with a fast and voltage-dependent rate of inactivation in both CHO and HEK cells. These results indicate that under the appropriate conditions Kv3.3 channels can exhibit fast and reliable inactivation that approaches that more typically expected of "A"-type K^+ currents.

Fast inactivating potassium channels play an important role in regulating neuronal output by setting the initial delay and frequency of spike discharge upon membrane depolarization (1). The expression pattern and kinetics of inactivating K^+ channels can also be controlled over the soma-dendritic axis of central neurons, allowing these channels to contribute to synaptic plasticity and the properties of backpropagating dendritic spikes (2–5). K^+ channel α-subunits can exhibit slow C- or fast N-type inactivation, the latter incorporating an NH_2-terminal "ball and chain" motif on the α-subunit to block the channel pore (6–8). Within the Kv1–4 families, fast inactivating K^+ channels include Kv1.4, 3.4, and all three members of the Kv4 family, while an intermediate rate of inactivation has been reported for Kv3.3 (9–11). The voltage dependence and rate of inactivation of these channel subtypes are critical to determining their contribution to neuronal excitability.

The inactivation properties of Kv1.4, Kv3.4, and Kv4.1–4.3 have all been well characterized in mammalian heterologous systems (12–15). While inactivating Kv3.3 channels have been successfully expressed in *Xenopus* oocytes (9) and more recently in Chinese hamster ovary (CHO)[1] cells (10), obtaining consistent inactivation of rat Kv3.3 has been difficult in the human embryonic kidney (HEK) cell expression system (16). Understanding the kinetic properties of Kv3.3 channels is important as this channel can be densely distributed over dendritic membranes of both principal cells and interneurons (17, 18). Moreover, a reduction in the contribution of these channels to dendritic spike repolarization has been shown to augment burst discharge in an electrosensory neuron (18). The rate of inactivation of Kv3.3 channels may even contribute to a dynamic modulation of dendritic refractory period during repetitive activity that underlies burst discharge (19).

We previously reported on some of the properties of teleost Kv3.3 channels (AptKv3.3) when expressed in tSA201 HEK cells and recorded in the outside-out patch configuration (18). However, as reported by others (16), the inactivation rate of Kv3.3 whole-cell currents in HEK cells often showed little or no inactivation during 100-ms step commands. The present study examined the kinetic properties of whole-cell currents of AptKv3.3 channels expressed in CHO and HEK cells. We find that AptKv3.3 cDNA gives rise to a fast inactivating whole-cell current in CHO but not HEK cells. By mutating nucleotides upstream of the first start site to one more closely resembling the optimal Kozak consensus sequence, both CHO and HEK cells express fast inactivating AptKv3.3 current. Under these conditions AptKv3.3 currents are capable of inactivating at rates that are close to that reported for even the fast inactivating mammalian Kv3.4.

EXPERIMENTAL PROCEDURES

Molecular Biology—Primers used to amplify the full coding region of AptKv3.3, including 10 base pairs of 5′-untranslated region (5′-UTR), have been described previously (18). In this study, the same AptKv3.3 cDNA was cloned into the expression vector pCDNA3.1 (Invitrogen)

* This work was supported by Canadian Institutes of Health Research grants (to R. W. T. and R. J. D.) and an Alberta Heritage Foundation for Medical Research Senior Scholarship (to R. W. T.). The costs of publication of this article were defrayed in part by the payment of page charges. This article must therefore be hereby marked "*advertisement*" in accordance with 18 U.S.C. Section 1734 solely to indicate this fact.

¶ To whom correspondence should be addressed: Neuroscience Research Group, University of Calgary, 3330 Hospital Dr. N.W., Calgary, Alberta T2N 4N1, Canada. Tel.: 403-220-8452; Fax: 403-283-2700; E-mail: rwturner@ucalgary.ca.

[1] The abbreviations used are: CHO, Chinese hamster ovary; HEK, human embryonic kidney; UTR, untranslated region; GFP, green fluorescent protein; TEA, tetraethylammonium; S, siemens; IRES, internal ribosome entry site.

using *Xho*I and *Xba*I restriction sites present in the forward and reverse primers, respectively.

To generate an AptKv3.3 expression construct in which the Kozak sequence around the initiation methionine was altered (AptKv3.3*Koz*), a fragment of cDNA encompassing nucleotides −6 to 628 of AptKv3.3 was PCR amplified from an AptKv3.3 expression construct. The following primers were used: forward, 5′ (CAC TCG AGC CGC CAT GCT CAG TTC CGT GTG TG); reverse, 5′ (TAG CGG GCA TAT TTA GAG GAG TAG). The forward primer contained the altered sequence GCC GCC preceding the methionine codon and an *Xho*I at the 5′ end for subcloning. The PCR fragment encompassed an *Apa*I restriction site normally present in AptKv3.3 cDNA at position 590. After amplification, the PCR fragment was digested with *Xho*I and *Apa*I restriction enzymes and substituted for the *Xho*I-*Apa*I fragment present in the original AptKv3.3 expression vector. The presence of the altered Kozak sequence was confirmed by DNA sequencing. The amino-terminal truncated AptKv3.3 cDNA was prepared by replacement of the cDNA encoding amino acids 1–27 with the coding sequence of enhanced GFP in the expression vector pEGFP-C1 (Clontech).

Sequences for mouse, rat, and human Kv3.3 and Kv3.4 sequences were obtained from the GenBank™ data base. Accession numbers are as follows: AptKv3.3 (AF308934), rKv3.3a, rKv3.3b, rKv3.3c, and rKv3.3d (rKv3.3a, M84210; rKv3.3b, M84211; rKv3.3c, AY179603.1; rKv3.3d, AY179604.1), mKv3.3b (NM_008422), hKv3.3a (AF055989), rKv3.4a (X62841), hKv3.4a and hKv3.4b (hKv3.4a, NM_004978; hKv3.4b, NM_153763).

Heterologous Expression of AptKv3.3—HEK cells were maintained in Dulbecco's modified Eagle's medium (Invitrogen) supplemented by 10% fetal bovine serum and 1% penicillin-streptomycin. CHO (CHO-K1; ATTC CLL-61) were maintained in F-12K medium (Kaighn's modification) (Invitrogen) supplemented by 10% fetal bovine serum and 1% penicillin-streptomycin. All cultures were kept at 37 °C. Cells were plated onto glass coverslips and co-transfected with 5 μg of AptKv3.3 vector cDNA and 1.0 μg of eGFP-C1 (Invitrogen) using 50 ml of 2.5 M $CaCl_2$ per 35-mm dish at 70% confluence. CHO cells were plated onto glass coverslips and co-transfected with 1.25 μg of AptKv3.3 vector cDNA and 0.7 μg of eGFP-C1 using 7.5 μl of Polyfect (Qiagen, Valencia, CA) per 35-mm dish at 70% confluence. All chemicals were obtained from BDH (Darmstadt, Germany) or Sigma unless otherwise indicated.

Electrophysiology—Patch electrodes were constructed from borosilicate glass (2.0 mm outer diameter or fiber-filled 1.5 mm outer diameter) (A-M Systems, Carlsborg, WA) using a Sutter P-87 microelectrode puller. Recordings were obtained using an Axopatch 200-A or Axopatch 1-D amplifier and PClamp 8 software (Axon Instruments, Foster City, CA) and data stored on a PC for later analysis. Seals were typically 1.5 GΩ or greater, and any leak current in whole-cell or outside-out mode was subtracted on-line. Electrode resistance was 2–5 MΩ with series resistance of 5–15 MΩ corrected by series resistance compensation at 80–90%. The electrolyte consisted of (in mm): KCl, 144; Hepes, 5; $MgCl_2$, 1; EGTA, 5; Mg-ATP, 1.5; 0.1, $CaCl_2$; pH 7.2. Whole-cell recordings were acquired at 1–2 kHz and single channel recordings in the on-cell or outside-out configuration were acquired at 2–5 kHz and digitally filtered during analysis at 1–2 kHz.

Coverslips containing cells were mounted on the stage of an upright submerged lens (Zeiss Axioskop I) or inverted microscope (Olympus) and perfused at room temperature with a medium consisting of (mM): NaCl, 148; Hepes, 10; $K_2H_2PO_4$, 1.25; KCl, 2; $CaCl_2$, 1.5; $MgCl_2$, 1.5; D-glucose, 20; pH 7.4. Recordings were typically obtained 48–72 h after transfection of cells and identified by GFP fluorescence. The rate of transfection as judged by GFP fluorescence was typically 1–2%, with the vast majority of fluorescing cells expressing AptKv3.3 current. Recordings were restricted to cells expressing 1.5–8 nA whole-cell current when stepped from −90 to +50 mV. Whole-cell control recordings in non-transfected HEK cells yielded background K^+ currents <300 pA and in CHO cells <25 pA. Our cell line gave no evidence for the range of potential K^+ currents suggested by a recent PCR analysis of another 293 cell line (20).

Calculations—Conductance was calculated as $g = I/(V - E_K)$ normalized to the maximum conductance, using an experimentally derived K^+ reversal potential of −95 mV. Conductance and inactivation plots were fit to a Boltzmann equation as follows,

$$I(V) = \frac{A_1 - A_2}{1 + e^{(V - V_{1/2})/k}} + A_2 \quad \text{(Eq. 1)}$$

where V = voltage, and k = slope factor.

The data points of TEA effects were fit to calculate IC_{50} using the following logistic function,

$$I(x) = \frac{A_1 - A_2}{1 + (x/x_0)^p} + A_2 \quad \text{(Eq. 2)}$$

where x = TEA concentration and p is the equivalent Hill coefficient. Activation τ was calculated between the end of the compensated capacitive transient and the peak current using a single exponential fit raised to a power of 4 (see Equation 3).

$$I(t) = A_1(1 - e^{(-t/\tau_1)})^4 \quad \text{(Eq. 3)}$$

Inactivation τ was calculated from the peak of the evoked current to a point corresponding to steady-state inactivation and deactivation τ from the peak of the tail current to steady-state. Exponential fits were used and calculated using the following equation.

$$I(t) = A_1 e^{(-t/\tau_1)} \quad \text{(Eq. 4)}$$

Plots of the voltage dependence of activation τ were fit using the following equation,

$$\tau(V) = A_1 e^{(Vq/kT)} \quad \text{(Eq. 5)}$$

where q is apparent charge associated with τ. Plots of the voltage dependence of inactivation τ (τ_v) were fit using the following equation.

$$\tau(V) = A_1 e^{(-V/\tau_v)} \quad \text{(Eq. 6)}$$

The time course of recovery from inactivation was fit using a single exponential function (see the following equation).

$$I(t) = A_1(1 - e^{(-t/\tau_1)}) \quad \text{(Eq. 7)}$$

Origin 7.1 (Microcal, Northampton, MA) and Clampfit 8.2 (Axon Instruments, Foster City, CA) were used for fitting. Statistical significance was determined using a two-sample Student's t test. Average values are expressed as mean ± S.E.

RESULTS

Current Activation and Deactivation—The majority of recordings were made in the whole-cell mode from AptKv3.3 channels expressed in CHO or HEK cells. Step commands from a holding potential of −90 mV in 10 mV depolarizing steps revealed an outward rectifying current that first became apparent for steps between −30 to −10 mV (Fig. 1*A*). Activation of the current in both expression systems was fast in exhibiting a τ for activation of <1.2 ms for steps from −90 to 30 mV (Table I). The τ for the rising phase of activation decreased with increasing voltage steps (Fig. 1*B*) but was significantly slower in CHO than HEK cells, with the greatest difference at low voltages. Once above activation voltage, plots of evoked current rose in a linear fashion with no reduction of current at higher voltages, as reported for some expressed Kv3 channels (9, 21). The voltage for activation plots for AptKv3.3 in CHO and HEK cells could be superimposed (Fig. 1*C*), with a $V_{1/2} = 7.6 \pm 0.8$ mV for CHO cells and 8.2 ± 0.8 mV for HEK cells (Table I).

Deactivation was rapid in both CHO and HEK cells (CHO τ = 0.55 to 1.09 ms; HEK τ = 0.41 to 0.81 ms) and voltage-dependent between −80 and −30 mV (Fig. 1, *D* and *E*). As found for activation, the τ of deactivation in CHO cells was significantly slower than that in HEK cells. The single channel slope conductance measured under presumed equimolar K^+ in the on-cell configuration ranged between 32 and 38 pS and was not significantly different for channels expressed in CHO or HEK cells (Fig. 1*F*; see also Table I).

As reported previously for mammalian Kv3.1 (22), initial activation of AptKv3.3 in HEK cells could be accompanied by an early transient peak of current but less so when expressed in CHO cells. This early peak in HEK cells has been attributed to a transient shift in extracellular K^+ concentration (22). The

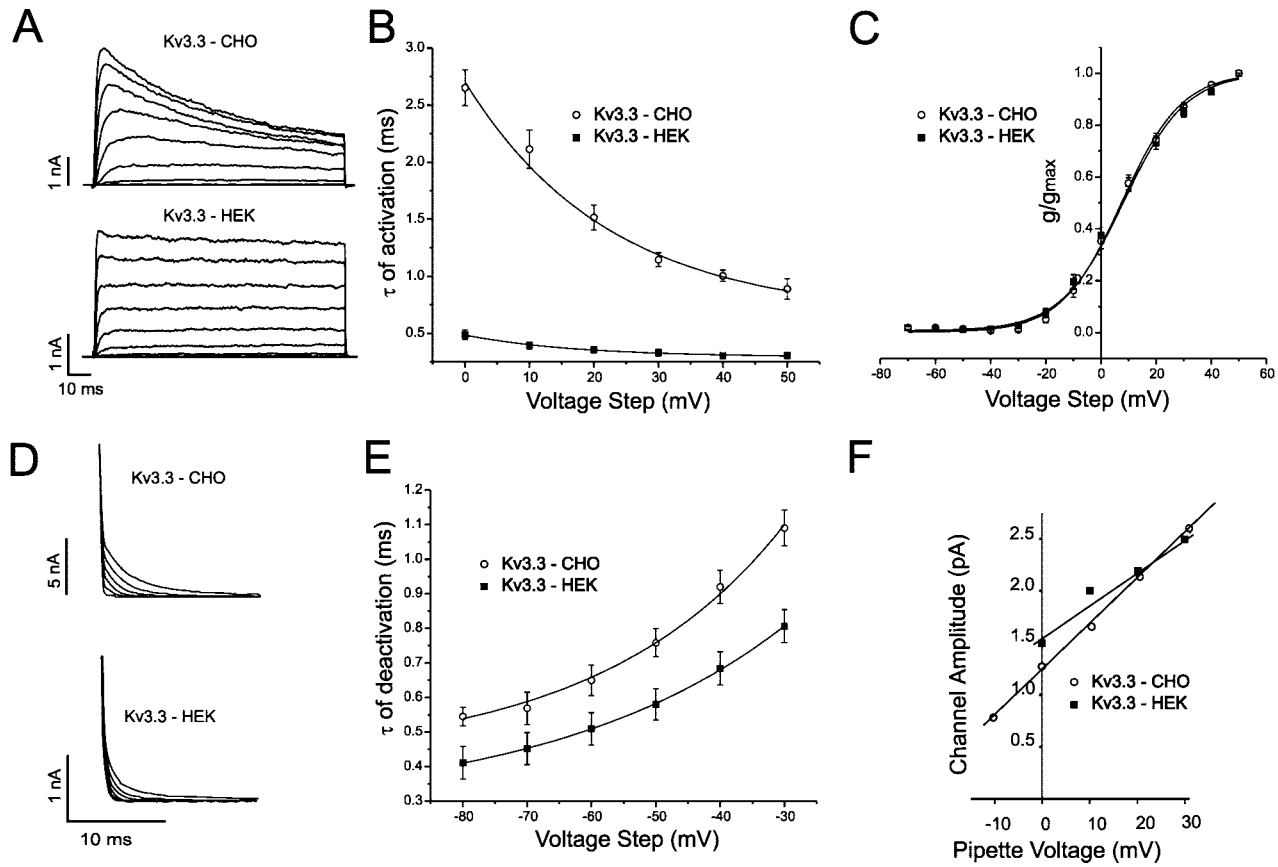

FIG. 1. **Activation, deactivation, and conductance properties of AptKv3.3 channels expressed in CHO and HEK cells.** All plots are indicated as CHO (○) or HEK (■) cell data. *A–C*, representative whole-cell current traces of AptKv3.3 for activation (*A*), plots of the voltage dependence of the time constant (τ) for the rising phase of current activation (*B*), and the voltage dependence of conductance (*C*). For the activation protocol cells were held at −90 mV and stepped to 50 mV in 10 mV increments for 100 ms. The τ for activation time (*B*) was determined using a single exponential function raised to the power of 4. The voltage dependence for τ of activation was significantly different between CHO and HEK cells ($p < 0.05$; $n = 8$) for all voltages indicated and fit using Equation 5 (see "Results") with apparent charge (q) values of $1.20e_0$ for CHO cells and $1.44e_0$ for HEK cells. The voltage dependence of conductance (*C*) was not significantly different ($n = 7$ CHO, $n = 9$ HEK). Data points in *C* were fit with Boltzmann functions. *D* and *E*, representative whole-cell current traces of AptKv3.3 deactivation (*D*) and plots of the voltage dependence of τ for deactivation (*E*). For the deactivation protocol cells were held at −90 mV, stepped to 50 mV for 5 ms, and then stepped from −80 to −30 mV in 10-mV increments. The voltage dependence of deactivation was significantly different between CHO and HEK cells for all voltages indicated except −70 mV ($p > 0.05$; $n = 8$) and was fit with a single exponential function. *F*, representative plots of single channel slope conductance measured in on-cell recording mode with equimolar K^+ (144 mM) pipette solution in CHO ($\gamma = 40$ pS) and HEK ($\gamma = 35$ pS) cells (see Table I).

lower prevalence of this early peak in CHO cells may reflect the slower rate of activation, decreasing a putative increase in extracellular K^+ ions. This was supported by preventing the early peak of current in HEK cells using a 5 ms voltage ramp command from −90 to 50 mV (28 mV/ms; data not shown).

TEA Pharmacology—As found for other Kv3 subtypes, AptKv3.3 channels were highly sensitive to external TEA application (Fig. 2*A*) (16, 23). In both cell types, substantial block was obtained for whole-cell currents in the range of 200 μM TEA or less (Fig. 2*B*), with a distinct decrease in single channel conductance (Fig. 2*C*). There was a significantly lower IC_{50} for whole-cell currents expressed in CHO compared with HEK cells (Fig. 2*B*) (CHO $IC_{50} = 67.5 \pm 4.2$ μM, HEK $IC_{50} = 152 \pm 27$ μM). The IC_{50} value for TEA obtained in HEK cells was equivalent to that reported for Kv3.3a expressed in oocytes at 140 ± 43 μM (9). AptKv3.3 currents expressed in HEK cells were also highly sensitive to externally applied 4-AP ($IC_{50} < 100$ μM) (18).

Current Inactivation—Expression of AptKv3.3 cDNA produced currents in CHO and HEK cells that differed dramatically in their inactivation properties. In CHO cells AptKv3.3 current reliably inactivated, with a rate of decay that could be fit well with a single exponential (Fig. 3, *A* and *B*). The τ of inactivation was voltage-dependent in decreasing at higher voltage steps from 251 ± 33.5 ms at 0 mV to 84 ± 14.0 ms at 50 mV (Fig. 3*B*). By comparison, the same cDNA expressed in HEK cells produced slower inactivating currents. Furthermore, there was a high degree of variability in the rate of inactivation, in that approximately half the transfected HEK cell population showed little or no inactivation within 10 s or required step commands to greater than 100 mV from a holding potential of −90 mV before any inactivation could be observed. Our analysis in HEK cells was restricted to those recordings reaching steady-state inactivation within 10 s for steps from −90 to 50 mV. This group presented a slow and voltage-independent inactivation that could only be fit with two exponentials (Fig. 3, *D* and *E*). An initial τ for inactivation in HEK cells ranged from 96.8 ± 17.7 to 132.8 ± 35 ms and a second τ from 1037.5 ± 215.7 ms to 1682.2 ± 526.2 ($n = 9$). The $V_{½}$ for inactivation in HEK cells was significantly left-shifted compared with CHO cells, with a value of -30.0 ± 0.86 mV compared with -22.5 ± 0.7 mV in CHO cells (Fig. 3, *C* and *F*) (Table I). The rate of recovery of AptKv3.3 also differed between CHO and HEK cells (Fig. 3*G*), with a τ of recovery after steady-state inactivation of 255 ± 27 ms in CHO cells and 174 ± 21 ms in HEK cells (Table I).

The rate of inactivation of other mammalian K^+ channels can vary depending on such factors as the cytosolic content of

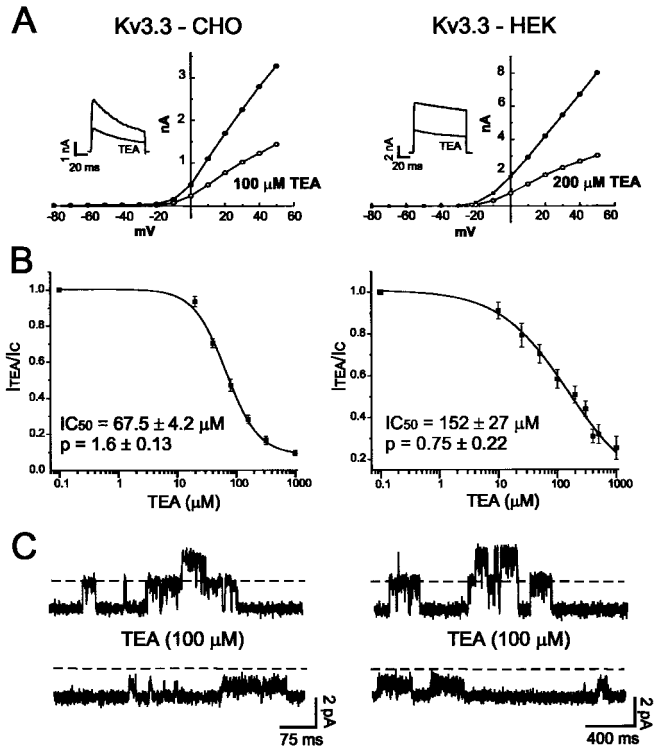

FIG. 2. **TEA sensitivity of AptKv3.3 expressed in CHO and HEK cells.** *A*, representative current-voltage relation before (●) and after (○) bath application of 100 and 200 μM TEA for AptKv3.3 expressed in CHO and HEK cells, respectively. *B*, TEA concentration dependence of AptKv3.3 current block in CHO and HEK cells with IC_{50} and p values that were significantly different ($p < 0.05$; $n = 6$ CHO, $n = 12$ HEK). Data points were fit with a logistic function. *C*, single channel amplitude reductions recorded in the outside-out configuration in the presence of 100 μM TEA in both expression systems. The *dashed lines* indicate the amplitude of channels openings in control conditions.

second messengers or redox environment (13, 24–28). These factors might then explain the different kinetics of AptKv3.3 observed in the two cell lines. To test this hypothesis we recorded AptKv3.3 currents in CHO and HEK cells in the outside-out configuration to maximize intracellular washout and reduce differences in cytosolic factors. We found in outside-out recordings that single channels of AptKv3.3 expressed in HEK cells showed a high steady-state open probability over 5 s, while those expressed in CHO cells showed clear inactivation and an extremely low steady-state open probability within 1 s (Fig. 3*H; n* = 10). In addition, macropatch recordings showed that large differences in the rate of inactivation persisted between CHO and HEK cells (Fig. 3*I*). These results indicate that the primary difference in the rate of inactivation between CHO and HEK cells does not likely arise from cytosolic factors.

Effects of Modifying the Kozak Consensus Sequence—The efficiency of translation at a methionine start site has been shown to depend on the resemblance of the nucleotide sequence surrounding the AUG start site with respect to an optimal Kozak consensus sequence (29). A Kozak consensus sequence consists of a purine (A/G) at position −3 relative to adenine of the methionine mRNA codon (AUG) and/or a guanine at position +4. An ideal Kozak consensus sequence will incorporate both of these features, although only one is required to initiate translation at an AUG codon. mRNA sequences not corresponding closely to the Kozak consensus sequence can lead to leaky scanning, in which the ribosome does not begin translation at a given potential methionine start site (29, 30).

The mRNA sequence for mammalian Kv3.3 channels has been shown to contain two putative methionine start sites at the 5′ end (9, 10, 16). It has been suggested that translation from the different start sites could explain the differences in inactivation observed between Kv3.3 expressed in *Xenopus* oocytes and HEK cells (16). Similarly, in AptKv3.3 a second methionine in the open reading frame can be found 29 amino acids downstream from the first methionine, at the end of the putative inactivation domain (Fig. 4*A*). If translation started from the second methionine codon, the resulting currents encoded by the truncated isoform would presumably be lacking fast NH_2-terminal-mediated inactivation, potentially accounting for the slower rate of inactivation in HEK cells. This hypothesis is strengthened by the observation that the nucleotide sequence surrounding the first methionine codon in AptKv3.3 does not match the Kozak consensus sequence for translation initiation (29). To examine whether preferential translation from the first methionine codon could increase the rate of inactivation of AptKv3.3, the six nucleotides preceding the first methionine codon were replaced with the sequence (gcc gcc) to provide a closer fit to the Kozak consensus sequence (AptKv3.3*Koz*) (Fig. 4*B*). The cytosine nucleotide at position +4 was not changed to the Kozak consensus of guanine, because it would change the amino acid at this position from leucine to valine. A second cDNA without the coding region for the first 29 amino acids was also produced (AptKv3.3Δ*1–29*) to test the result of removing the NH_2-terminal region on whole-cell currents.

Inactivation of the Kozak-modified Constructs—Whole-cell recordings from AptKv3.3*Koz* expressed in CHO cells generated currents that inactivated with an average τ that was 40% faster at 30 mV than those generated from the unmodified AptKv3.3 expression vector (Fig. 5*A*). Expression from the AptKv3.3*Koz* vector in HEK cells now consistently produced a very fast inactivating current, exhibiting a τ that was 52% faster than even AptKv3.3*Koz* expressed in CHO cells (Fig. 5, *A* and *B*). By comparison, expression of AptKv3.3Δ*1–29* resulted in a non-inactivating current with a similar profile to the original AptKv3.3 construct expressed in HEK cells, including a prominent transient peak of current often attributed to fast activation and extracellular K^+ accumulation (Fig. 5*A*). The τ of AptKv3.3*Koz* inactivation was also voltage-dependent in both cell lines, ranging from 130 ± 12.0 ms at 0 mV to 52.9 ± 3.7 ms at 50 mV in CHO cells compared with 52.1 ± 5.0 ms at 0 mV to 25.4 ± 2.0 ms at 50 mV in HEK cells (Fig. 5*B*; see also Table I).

AptKv3.3*Koz* in CHO cells showed a similar $V_{1/2}$ of inactivation and k value to that of AptKv3.3 (*cf.* Figs. 5*D* and 3*C*). In HEK cells both the $V_{½}$ of inactivation and k value for AptKv3.3*Koz* were significantly altered compared with the unmodified AptKv3.3 (*cf.* Figs. 5*E* and 3*F*) but to final values that were not significantly different from those in CHO cells. Recovery from inactivation was significantly lengthened when AptKv3.3*Koz* was expressed in HEK cells over that of AptKv3.3 (Fig. 5*F*). However, recovery from inactivation was not significantly different between those constructs predicted to express NH_2-terminal regions (AptKv3.3 in CHO and AptKv3.3*Koz* in CHO and HEK cells) (Fig. 5*F*).

The τ for activation of AptKv3.3*Koz* in HEK cells was significantly slower at all voltages compared with those expressed from the unmodified AptKv3.3 construct (Fig. 5*C*) but more similar to that of AptKv3.3*Koz* in CHO cells (Fig. 5*C*). Removal of the NH_2 terminus in AptKv3.3Δ*1–29* resulted in a significant increase in the rate of activation compared with the fast inactivating channels, with an activation profile very similar to the slow inactivating AptKv3.3 expressed in HEK cells. The $V_{½}$ for activation was also negative-shifted for AptKv3.3*Koz* channels expressed in CHO or HEK cells compared with AptKv3.3, with a shift of −4.2 mV in CHO cells and −10.6 mV in HEK cells (*cf.*

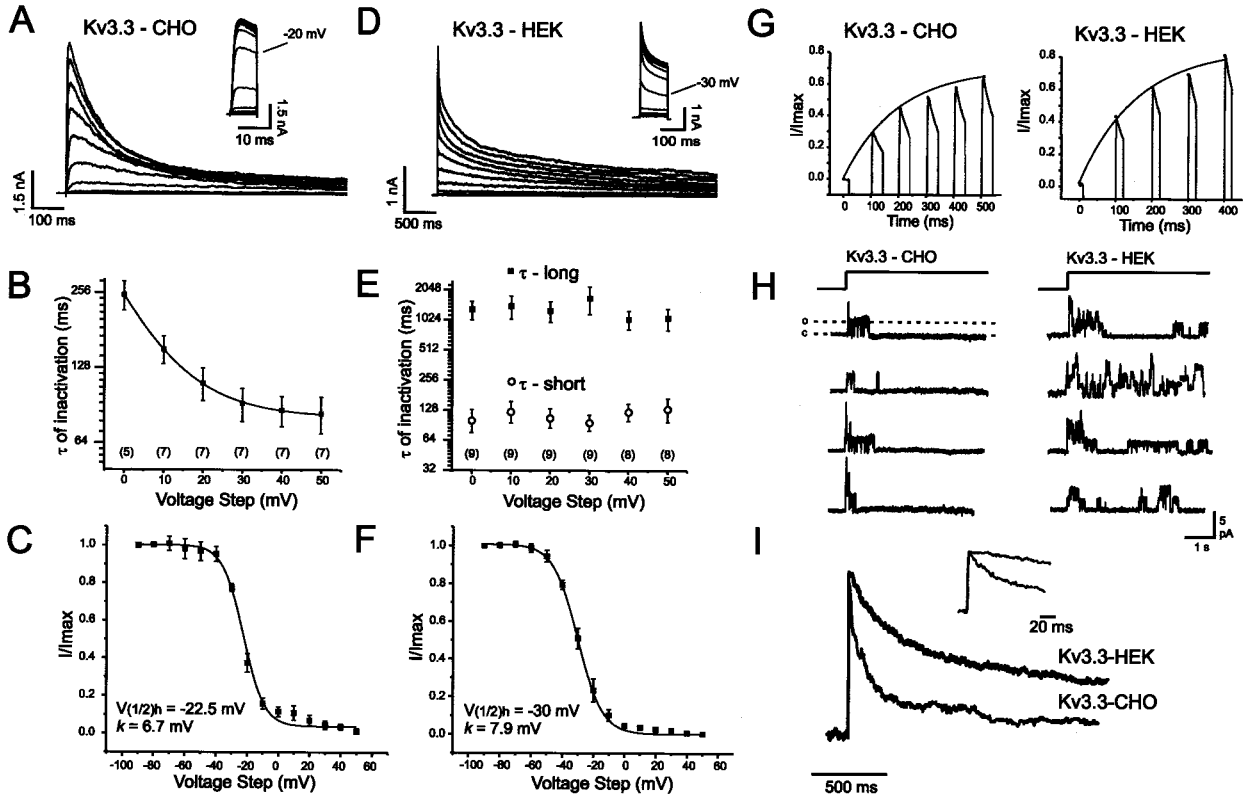

FIG. 3. **Inactivation kinetics of AptKv3.3 differ in CHO and HEK cells.** Kinetics of inactivation in CHO (*A–C*) and HEK (*D–F*) cells. *A* and *D*, representative current traces of AptKv3.3 indicating fast inactivation in CHO and slow inactivation in HEK cells (note difference in time scales). For AptKv3.3 expressed in CHO cells, cells were held at −90 mV and stepped to 50 mV in 10-mV increments for 4 s, followed by a test pulse to 50 mV for 10 ms (*inset*). For AptKv3.3 expressed in HEK cells, the cell was held at −90 mV and stepped to 50 mV in 10-mV increments for 10–25 s, followed by a test pulse to 50 mV for 80 ms (*inset*). *B* and *E*, voltage dependence of inactivation time constants (τ). AptKv3.3 current inactivation was fit with a single exponential function in CHO cells and by a double exponential function in HEK cells. The τ of inactivation was voltage-dependent in CHO cells, and the relationship was fit with a single exponential decay function (*B*), while both the short (τ_{short}) and long (τ_{long}) time constants in HEK cells were voltage-independent (*E*). *C* and *F*, steady-state inactivation curves for AptKv3.3. The $V_{½}$ and k value of inactivation were significantly different for CHO and HEK cells ($p < 0.05$; $n = 5$ CHO, $n = 9$ HEK). Data points were fit with Boltzmann functions. *G*, time course of recovery from inactivation in CHO and HEK cells. The τ of recovery of control current was significantly longer in CHO than in HEK cells ($p < 0.05$; $n = 5$ CHO, $n = 7$ HEK). The τ of recovery was determined by depolarizing the cells to 50 mV from a holding potential of −90 mV until steady-state inactivation was reached. A step to −90 mV of variable duration was followed with test pulses to 50 mV for 10 ms in increments of 100 ms. Data points were fit with a single exponential function. *H*, outside-out patches containing two to four AptKv3.3 channels expressed in CHO or HEK cells. Shown are individual traces obtained from a holding potential of −70 mV stepped to 10–30 mV. *I*, comparison of inactivation rates in CHO and HEK cells in the outside-out recording configuration with a step from −90 to 50 mV revealed similar differences as found for whole-cell currents. The same traces are shown but at a smaller time scale in the *inset*. Traces have been normalized in current amplitude for comparison, with the initial 100 ms of recording shown in the *inset*.

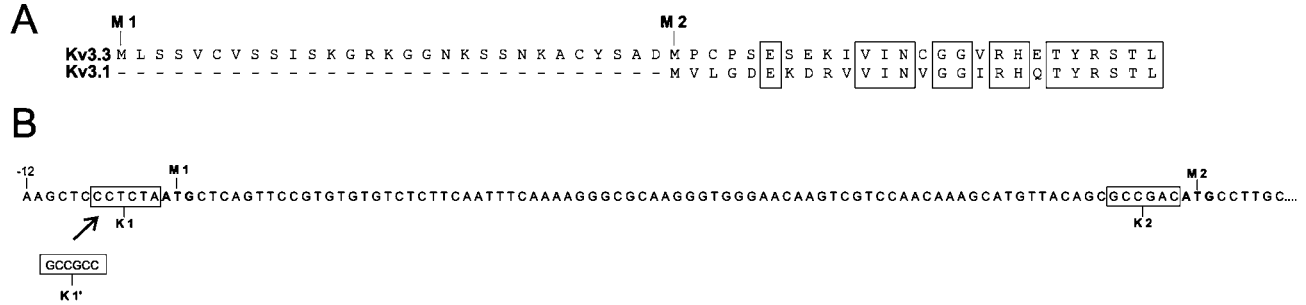

FIG. 4. **Mutation of the AptKv3.3 start sequence to a Kozak consensus sequence.** *A*, AptKv3.3 channels contain two putative methionine start sites for translation, M1 and a second (M2) 29 amino acids downstream. Sequence alignment with AptKv3.1 indicates that M2 of AptKv3.3 is at a position corresponding to the initiation methionine of AptKv3.1, past the putative inactivation domain of AptKv3.3 (amino acids 1–29). *Boxed regions* indicate identical amino acid sequences between AptKv3.3 and AptKv3.1. *B*, the sequence surrounding the M2 site represents a better Kozak consensus sequence for translation initiation than M1, possibly leading to leaky scanning by ribosomes to initiate translation at M2. *Boxed regions* indicate the six nucleotides preceding the ATG start sites at M1 (*K1*) and M2 (*K2*). To test whether an improved Kozak sequence at K1 would alter the rate of inactivation of whole-cell currents, we mutated the preceding six nucleotides to those shown in the K1′ *box*.

Fig. 5, *D* and *E*, and Fig. 1*C*; see also Table I). The k values associated with activation did not differ significantly between *Koz*-modified and unmodified currents. The $V_{½}$ for activation of AptKv3.3Δ*1–29* was 6.9 ± 1.3 mV with a k value of 14.0 ± 1.1mV in CHO cells, which was not significantly different from the original AptKv3.3 expressed in CHO or HEK cells. These results suggest that the presence of the inactivation particle can interact with the activation gate to slow the rise time and slightly shift the voltage dependence of activation.

In summary, the net result of mutating the Kozak consensus

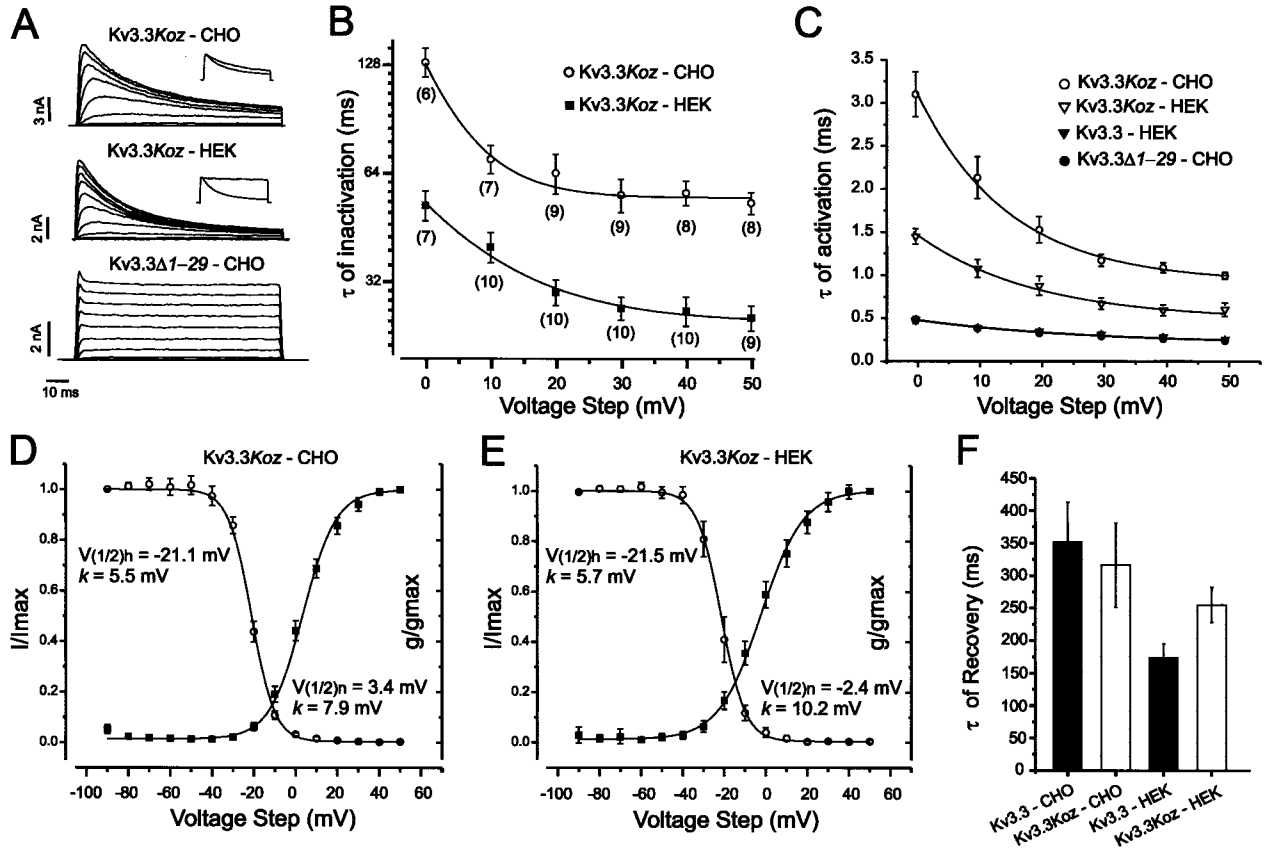

FIG. 5. **Activation and inactivation kinetics AptKv3.3*Koz*.** *A*, representative traces of AptKv3.3*Koz* expressed in CHO and HEK cells, illustrating fast inactivation in both cell types. The *lower trace* shows currents evoked after expressing a truncated version of AptKv3.3 cDNA in CHO cells designed to initiate translation at the second methionine codon and without the NH_2-terminal region (AptKv3.3Δ*1–29*). Voltage protocols are as described in the legend to Fig. 1*A*. *B*, voltage dependence of inactivation time constants (τ) for AptKv3.3*Koz*. Inactivation rates were fit with a single exponential function in both CHO (○) and HEK (■) cells. *C*, voltage dependence of the τ for activation of AptKv3.3*Koz* currents evoked from 0 to 50 mV in CHO (○) and HEK (▽) cells. The equivalent plot for the unmodified AptKv3.3 in HEK cells (▼) and AptKv3.3Δ*1–29* (●) constructs are shown for comparison. The τ of AptKv3.3*Koz* activation is significantly different between the expression systems for all voltages indicated ($p < 0.05$, $n = 6$ CHO, $n = 7$ HEK). The voltage dependence for τ of activation for AptKv3.3*Koz* CHO, AptKv3.3*Koz* HEK, and AptKv3.3Δ*1–29* were fit using Equation 5 (see "Results") with apparent charge (q) values of $1.68e_0$, $1.33e_0$, and $1.90e_0$, respectively. *D* and *E*, voltage dependence of conductance (■) and steady-state inactivation (○) curves for AptKv3.3*Koz* expressed in CHO (*D*) and HEK (*E*) cells. The $V_{½}$ of activation was significantly different between AptKv3.3*Koz* expressed in CHO and HEK cells ($n = 7$ CHO, $n = 8$ HEK; $p < 0.05$), while steady-state inactivation curves were not significantly different ($n = 5$ CHO, $n = 7$ HEK). Data points were fit with Boltzmann functions. *F*, the τ for recovery from inactivation was significantly longer in AptKv3.3*Koz* compared with AptKv3.3 in HEK cells ($p < 0.05$, $n = 7$ Kv3.3, $n = 4$ Kv3.3*Koz*) but did not change significantly in CHO cells between the two constructs. The τ for recovery between CHO cells and AptKv3.3*Koz* in HEK cells was also not significantly different. The protocol followed the same procedure as that described for Fig. 3*G*.

sequence preceding M1 was to produce currents that inactivated more rapidly with identical voltage dependence and at a rate that could be fit with a single exponential in both CHO and HEK cells.

DISCUSSION

This study establishes the kinetic properties of AptKv3.3 channels when expressed in two mammalian cell lines. Although several properties of activation, deactivation, and conductance were equivalent in the two systems, we encountered key differences in the properties of inactivation. The most significant difference was a fast inactivation when expressed in CHO cells but only slow inactivation in HEK cells, as reported previously for mammalian Kv3.3 in HEK cells (16). These differences could be due to posttranslational modifications or even translational differences that affect channel structure. The potential influence of second messengers on channel inactivation was tested by recording AptKv3.3 currents in the outside-out configuration. Since large differences in the rate of inactivation persisted under conditions expected to promote substantial washout through dialysis by the electrode, cytosolic factors could not account for the major differences in inactivation rates. A more important role was identified in the translational process with respect to successful translation of an NH_2-terminal domain.

Others have identified two potential methionine start sites for translation in the NH_2-terminal region of mammalian Kv3.3 and Kv3.4 channels (16). Inspection of AptKv3.3 revealed that the first of two potential start sites lacked key nucleotides to meet the Kozak consensus requirement for efficient translation. Because the region between the two start sites codes for the putative fast inactivation particle of AptKv3.3, potential leaky scanning past the first start site could lead to translation of subunits with a truncated NH_2 terminus, a result predicted to influence inactivation characteristics. To test this we changed the nucleotide sequence preceding the first methionine to one more closely resembling a Kozak consensus sequence. We found that expression of AptKv3.3*Koz* in CHO and HEK cells largely eliminated differences in inactivation properties, promoting a fast inactivation in both cell lines.

The increased expression of inactivating currents with AptKv3.3*Koz* is consistent with an improved translation of NH_2-terminal domains. The slow rate of AptKv3.3 inactivation in HEK cells may then reflect a greater number of channels

TABLE I
Properties of AptKv3.3 and AptKv3.3Koz when expressed in CHO or HEK cells
Step potentials and *n* values are shown in parentheses. γ = on-cell single channel conductance.

	Activation τ (30 mV)	Activation $V_{½}$ and k	Inactivation τ (30 mV)	Inactivation $V_{½}$ and k	τ recovery (−90 mV)	γ
	ms	*mV*	*ms*	*mV*	*ms*	*pS*
Kv3.3-CHO	1.15 ± 0.06 (8)	7.6 ± 0.8 (7) k = 10.7 ± 0.7	92.0 ± 14 (7)	−22.5 ± 0.7 (5) k = 6.7 ± 0.6	255 ± 27 (5)	37.8 ± 2.8 (6)
Kv3.3-HEK	0.33 ± 0.03 (8)	8.2 ± 0.8 (9) k = 11.2 ± 0.5	τ_1 = 96.8 ± 18 τ_2 = 1682 ± 526 (9)	−30 ± 0.9 (9) k = 7.9 ± 0.5	174 ± 21 (7)	32.5 ± 2.0 (5)
Kv3.3K*oz*-CHO	1.18 ± 0.07 (6)	3.4 ± 0.9 (7)[a] k = 7.9 ± 0.6	55.7 ± 5.9 (9)[a]	−21.1 ± 0.6 (5) k = 5.5 ± 0.3	352 ± 61 (4)	32.3 ± 1.9 (4)
Kv3.3K*oz*-HEK	0.68 ± 0.06 (7)[b]	−2.4 ± 1.4 (8)[b] k = 10.2 ± 1.0	27 ± 1.9 (10)[b]	−21.5 ± 1.2 (7)[b] k = 5.7 ± 0.7[b]	316 ± 65 (4)[b]	35.0 ± 2.2 (7)

[a] $p < 0.05$ between data sets for AptKv3.3 in CHO cells.
[b] $p < 0.05$ between data sets for AptKv3.3 in HEK cells.

translated without the NH_2-terminal ball and chain motif. One can envision a population of channels that could range from homomeric combinations of subunits without any NH_2-terminal domains to heteromeric combinations with varying numbers of NH_2 terminus-containing subunits. In this regard, deletion-mutation analyses in *Shaker* B and Kv1.4 suggest that substantial inactivation can be achieved with even one N-ball in a tetramer and that the $V_{½}$ of inactivation is independent of the number of N-balls (12, 31, 32). Similarly, co-expression of the inactivating Kv3.1 channel with a lower density of the inactivating Kv3.4 channel in oocytes produced a fast inactivating channel, leading again to the suggestion that only one or a small number of NH_2 terminus-containing subunits from Kv3.4 can induce fast inactivation in the presumed heteromerized channels (16). The findings from each of these channel types would thus suggest that if even a small number of AptKv3.3 channels expressed in HEK cells were translated with an NH_2-terminal domain, one would predict a much faster rate of inactivation than what we observed under whole-cell recording conditions. In support of this, outside-out recordings revealed that AptKv3.3 channels exhibited clear inactivation only when expressed in CHO cells (Fig. 3*H*). It is also interesting that the slow inactivating AptKv3.3 expressed in HEK cells exhibited a negatively shifted $V_{½}$ of inactivation and a voltage-independent rate of inactivation, unlike all other expressed AptKv3.3 currents. Altogether these results imply an extremely low rate of NH_2-terminal domain translation of AptKv3.3 in HEK cells and a substantially different inactivation process that could include a greater contribution of slow pore-mediated C-type inactivation.

We also found that expressing fast inactivating currents lead to a significant decrease in the rate of activation. Conversely, deleting the NH_2 terminus of AptKv3.3 removed fast inactivation and increased the rate of activation. These results differ from a state-dependent model of inactivation, where the removal of inactivation reveals the slower and true steady state (33, 34). Removal of the NH_2 terminus in mammalian Kv3.4 produces currents that have a slower rate of rise compared with full-length sequences (13), a result that is compatible with a state-dependent model of inactivation. Our results suggest a more complex model for inactivation that may incorporate a greater voltage dependence in the inactivation process. We also found that the rate of inactivation was not the sole determinant of the activation rate, as AptKv3.3*Koz* in HEK cells had a faster rate of activation than AptKv3.3*Koz* in CHO despite having a faster rate of inactivation (Fig. 5, *A–C*). This suggests that the presence of the NH_2-terminal domain introduces additional modulatory sites that can differentially affect the rate of activation between expression systems.

Comparison with Mammalian Kv3 Currents—Overall the voltage dependence and single channel conductance of AptKv3.3 was similar to mammalian Kv3.3. AptKv3.3 showed the first measurable whole-cell current in I–V plots for steps between −30 and −10 mV. In CHO and HEK cells the $V_{½}$ for activation for modified and unmodified AptKv3.3 constructs ranged between −2 and 8 mV with k values of 7–11 mV. This compares reasonably to a range for the mammalian Kv3.3 channel $V_{½}$ of 7–12 mV and k values between 6 and 14 mV (9, 16, 35). Finally, our single channel conductance measured in on-cell mode fell between 32 and 38 pS, essentially identical to the 39 pS conductance reported for hKv3.3 under the same recording conditions (10).

AptKv3.3 channels differed, however, in exhibiting a much faster rate of activation and deactivation than mammalian Kv3.3 (9, 10). The rate of AptKv3.3 inactivation in CHO cells (τ = 85 ms at 50 mV) was also faster than mammalian Kv3.3 ($\tau \sim$ 120 ms at 50 mV) (9) and fell within the range reported for Kv1.4 (τ = 43–160 ms) (12, 14, 32). AptKv3.3*Koz* inactivation in CHO and HEK cells was even faster (τ = 25–53 ms at 50 mV) and thus close to the Kv3.4 channel (τ = 10–20 ms at 50 mV) (13, 16, 21). These differences could relate to the temperature dependence of channel kinetics, as our recordings at room temperature (21 °C) are reasonably close to the native environment in which apteronotid electric fish live (26 °C). By comparison, all kinetic analyses of mammalian Kv3.3 channels have been carried out at room temperature. The faster kinetics observed in AptKv3.3 channels may then reflect channel activity closer to the physiological condition.

AptKv3.3 channels have been shown to play a role in spike repolarization (18, 19), but the exact contribution will depend critically on the rate of activation with respect to spike duration. In this regard, the fast rate of activation of AptKv3.3 channels should enable a significant role in spike repolarization, as shown for ELL pyramidal cells (18). The fast rate of inactivation shown here further makes this channel a possible candidate for the dendritic current proposed to promote burst output in ELL pyramidal cells through a cumulative inactivation (19, 36).

Initiation of Translation—Mammalian Kv3.3 and Kv3.4 channels have all been shown to have two potential methionine start sites: the first site enabling translation of the putative inactivation domain and the second corresponding to that shared with the non-inactivating Kv3.1 and 3.2 channel subtypes (16). Examination of mammalian mRNA sequences reveals that all Kv3.3 and Kv3.4 splice isoforms entirely lack a Kozak consensus sequence near the first methionine site but do have one at the second methionine site (Fig. 6). A poorly defined start site at the first methionine in AptKv3.3 is thus a ubiquitous feature among the fast inactivating Kv3 K^+ channel subtypes.

The functional significance of this to translation of Kv3.3 channels and their inactivation rates *in vivo* is unknown. We

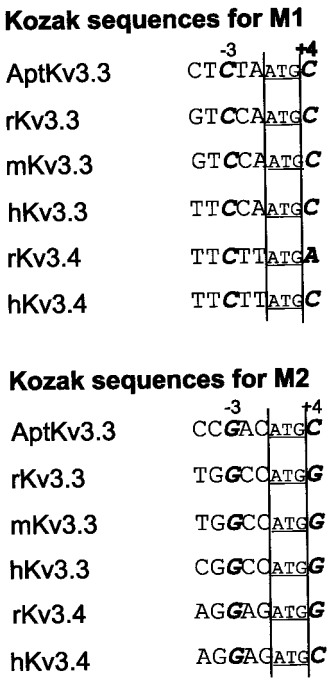

FIG. 6. **Comparison of Kv3.3 and Kv3.4 nucleotides surrounding the first (M1) and second (M2) putative start sites.** An ideal Kozak consensus sequence has a purine (A or G) at position −3 and a guanine at position +4, although translation can be initiated from an AUG codon that meets only one of the criteria. Examination of Kv3.3 and Kv3.4 start sequences shows that M1 is in an unfavorable context in all cases, while the M2 site meets the minimal requirements for a Kozak consensus site.

have previously recorded Kv3-like currents from ELL pyramidal cells (18). In the outside-out configuration, a single exponential fit procedure revealed an inactivation rate with a τ of ~250–450 ms at 0 mV (18), a rate of inactivation that is similar to that of AptKv3.3 whole-cell currents in CHO cells at the same voltage (~250 ms). Although we have shown that these currents do not correspond to dendrotoxin-sensitive Shaker-type K^+ channels or BK channels (19), we cannot entirely rule out an influence of a much lower expression level of Kv3.1 channels on the rate of inactivation.[2] However, the observed rate of inactivation in pyramidal cells at least indicates that translation of AptKv3.3 *in vivo* leads to channels with inactivation rates consistent with NH_2-terminal inactivation. A recent study also reported on the inactivation properties of Kv3-like channels in rat Purkinje cells, obtaining a fast inactivation component with a τ = 20 ms and a slow inactivation τ = 380 ms at 70 mV (3). Attributing these values to Kv3.3 channels is, however, more difficult given a high expression level of Kv3.4 and the expected presence of other K^+ currents under their recording conditions.

There is precedent for mRNA to contain multiple putative start sites and even for the initial start site to be regulated to determine the nature of the expressed protein (29, 37). Should leaky scanning occur at the first methionine start site of AptKv3.3 channels *in vivo*, one might expect some effect on inactivation according to the number of subunits in the final channel tetramer that include an NH_2 terminus. It is worth noting that fast inactivation can be achieved in Kv3.3 channels even if the Kozak sequence does not entirely match the optimal nucleotide sequence (as found for inactivation of AptKv3.3 in CHO cells; Fig. 3*A*). However, an improved Kozak consensus sequence can increase the rate of inactivation by at least 40%. Although it is interesting to speculate on the potential to regulate the rate of Kv3.3 inactivation according to the start site for translation, further studies will be required to determine the relevance of this for Kv3 channel proteins.

A second factor that could possibly regulate translation is the length of the 5′-UTR preceding the methionine start site (29, 30, 37). Rae and Shepherd (10) used a hKv3.3 with 485 base pairs of 5′-UTR and achieved fast inactivation in CHO cells, suggesting that the length of 5′-UTR could be important. In support of this, Rudy *et al.* (16) reported that the expression of Kv3.3 in CHO cells without an extended UTR produced a non-inactivating current. Our difficulty in expressing an inactivating AptKv3.3 current in HEK cells could then relate to the reduced length of the 5′-UTR in our unmodified cDNA (12 nucleotides). Nonetheless, this length of 5′-UTR was sufficient to produce a channel with fast inactivation in CHO cells. Studies of rat Kv3.2 and human Kv3.3 have further shown that multiple versions of cDNA sequences exist that differ in the length of their 5′-UTR, and that in rat, two different 5′-UTRs can be associated with more than one COOH-terminal splice isoform (35, 38). It has therefore been suggested that the 5′-UTR could represent a site for the production of multiple splice isoforms. Although this might include the regulation of the translation start site, the potential for the 5′-UTR to influence inactivation properties of Kv3.3 channels *in vivo* remains to be determined.

A final factor that could potentially influence the mRNA start site arises in the report of an internal ribosome entry site (IRES) in the 5′-UTR of Kv1.4 channels (39). A sequence compatible with an IRES was even noted for the mammalian Kv3.1 and 3.2 channel, although this was not examined for Kv3.3 (39). If these presumed IRES sites are functional, it could help account for why Kv3 channels have weak Kozak consensus sequences surrounding the initial methionine start site. However, given the requirements necessary to establish functionality at a potential IRES site (40), further work will be required to determine whether translation at Kv3.3 channels involves an IRES site.

In summary, the present study identifies one explanation for the variability in the rate of inactivation of Kv3.3 observed in previous studies and indicates that under the appropriate conditions Kv3.3 channels are capable of fast inactivation at rates that approach those of more traditional A-type K^+ currents.

Acknowledgments—We gratefully acknowledge the expert technical contributions of M. Kruskic and M. Lachance and R. J. French and G. W. Zamponi for comments on the manuscript.

REFERENCES

1. Connor, J. A., and Stevens, C. F. (1971) *J. Physiol.* (*Lond.*) **213,** 21–30
2. Johnston, D., Hoffman, D. A., Magee, J. C., Poolos, N. P., Watanabe, S., Colbert, C. M., and Migliore, M.(2000) *J. Physiol.* (*Lond.*) **525,** 75–81
3. **3** Martina, M., Yao, G. L., and Bean, B. P. (2003) *J. Neurosci.* **23,** 5698–5707
4. Watanabe, S., Hoffman, D. A., Migliore, M., and Johnston, D. (2002) *Proc. Natl. Acad. Sci. U. S. A.* **99,** 8366–8371
5. Migliore, M., Hoffman, D. A., Magee, J. C., and Johnston, D. (1999) *J. Comput. Neurosci.* **7,** 5–15
6. Hoshi, T., Zagotta, W. N., and Aldrich, R. W. (1990) *Science* **250,** 533–538
7. Hoshi, T., Zagotta, W. N., and Aldrich, R. W. (1991) *Neuron* **7,** 547–556
8. Zagotta, W. N., and Aldrich, R. W. (1990) *J. Gen. Physiol.* **95,** 29–60
9. Vega-Saenz de Miera, E., Moreno, H., Fruhling, D., Kentros, C., and Rudy, B. (1992) *Proc. R. Soc. Lond. B Biol. Sci.* **248,** 9–18
10. Rae, J. L., and Shepard, A. R. (2000) *Exp. Eye Res.* **70,** 339–348
11. Coetzee, W. A., Amarillo, Y., Chiu, J., Chow, A., Lau, D., McCormack, T., Moreno, H., Nadal, M. S., Ozaita, A., Pountney, D., Saganich, M., Vega-Saenz de Miera, E., and Rudy, B. (1999) *Ann. N. Y. Acad. Sci.* **868,** 233–285
12. Hashimoto, Y., Nunoki, K., Kudo, H., Ishii, K., Taira, N., and Yanagisawa, T. (2000) *J. Biol. Chem.* **275,** 9358–9362
13. Covarrubias, M., Wei, A., Salkoff, L., and Vyas, T. B. (1994) *Neuron* **13,** 1403–1412
14. Petersen, K. R., and Nerbonne, J. M. (1999) *Pflügers Arch.* **437,** 381–392
15. Franqueza, L., Valenzuela, C., Eck, J., Tamkun, M. M., Tamargo, J., and Snyders, D. J. (1999) *Cardiovasc. Res.* **41,** 212–219
16. Rudy, B., Chow, A., Lau, D., Amarillo, Y., Ozaita, A., Saganich, M., Moreno, H., Nadal, M. S., Hernandez-Pineda, R., Hernandez-Cruz, A., Erisir, A.,

[2] A. J. Rashid and R. J. Dunn, unpublished observations.

Leonard, C., and Vega-Saenz de Miera, E. (1999) *Ann. N. Y. Acad. Sci.* **868,** 304–343
17. Rashid, A. J., Dunn, R. J., and Turner, R. W. (2001a) *J. Comp. Neurol* **441,** 234–247
18. Rashid, A. J., Morales, E., Turner, R. W., and Dunn, R. W. (2001b) *J. Neurosci.* **21,** 125–135
19. Noonan, L., Doiron, B., Laing, C., Longtin, A., and Turner, R. W. (2003) *J. Neurosci.* **23,** 1524–1534
20. Jiang, B., Sun, X., Cao, K., and Wang, R. (2002) *Mol. Cell. Biochem.* **238,** 69–79
21. Rettig, J., Wunder, F., Stocker, M., Lichtinghagen, R., Mastiaux, F., Beckh, S., Kues, W., Pedarzani, P., Schroter, K. H., Ruppersberg, J. P., Veh, R., and Pongs, O. (1992) *EMBO J.* **11,** 2473–2486
22. Critz, S. D., Wible, B. A., Lopez, H. S., and Brown, A. M. (1993) *J. Neurochem.* **60,** 1175–1178
23. Rudy, B., and McBain, C. J. (2001) *TINS* **24,** 517–526
24. Velasco, I., Beck, E. J., and Covarrubias, M. (1998) *Neurobiology* (*BP*) **6,** 23–32
25. Drain, P., Dubin, A. E., and Aldrich, R. W. (1994) *Neuron* **12,** 1097–1109
26. Jonas, E. A., and Kaczmarek, L. K. (1996) *Curr. Opin. Neurobiol.* **6,** 318–323
27. Ruppersberg, J. P., Stocker, M., Pongs, O., Heinemann, S. H., Frank, R., and Koenen, M. (1991) *Nature* **352,** 711–714
28. Roeper, J., Lorra, C., and Pongs, O. (1997) *J. Neurosci.* **17,** 3379–3391
29. Kozak, M. (1999) *Gene* (*Amst.*) **234,** 187–208
30. Kozak, M. (1996) *Mamm. Genome* **7,** 563–574
31. MacKinnon, R., Aldrich, R. W., and Lee, A. W. (1993) *Science* **262,** 757–759
32. Lee, T. E., Philipson, L. H., and Nelson, D. J. (1996) *J. Membr Biol* **151,** 225–235
33. Aldrich, R. W., Corey, D. P., and Stevens, C. F. (1983) *Nature* **306,** 436–441
34. Zagotta, W. N., Hoshi, T., and Aldrich, R. W. (1989) *Proc. Natl. Acad. Sci. U. S. A.* **86,** 7243–7247
35. Vega-Saenz de Miera, E., Weiser, M., Kentros, C., Lau, D., Moreno, H., Serodio, P., and Rudy, B. (eds) (1994) *Handbook of Membrane Channels* (Edited by Peracchia, C., ed) pp. 41–78, Academic Press, Orlando, FL
36. Doiron, B., Longtin, A., Turner, R. W., and Maler, L. (2001) *J. Neurophysiol.* **86,** 1523–1545
37. Descombes, P., and Schibler, U. (1991) *Cell* **67,** 569–579
38. Kentros, C., Weiser, M., Vega-Saenz de Miera, E., Morel, K., Baker, H., and Rudy, B. (1992) *Soc. Neurosci. Abstr.* **18,** 1093
39. Negulescu, D., Leong, L. E., Chandy, K. G., Semler, B. L., and Gutman, G. A. (1998) *J. Biol. Chem.* **273,** 20109–20113
40. Kozak, M. (2001) *Mol. Cell. Biol.* **21,** 1899–1907